

This work was written as part of one of the author's official duties as an Employee of the United States Government and is therefore a work of the United States Government. In accordance with 17 U.S.C. 105, no copyright protection is available for such works under U.S. Law.

Public Domain Mark 1.0

<https://creativecommons.org/publicdomain/mark/1.0/>

Access to this work was provided by the University of Maryland, Baltimore County (UMBC) ScholarWorks@UMBC digital repository on the Maryland Shared Open Access (MD-SOAR) platform.

Please provide feedback

Please support the ScholarWorks@UMBC repository by emailing scholarworks-group@umbc.edu and telling us what having access to this work means to you and why it's important to you. Thank you.



Resonant tidal excitation of internal waves in the Earth's fluid core



Robert H. Tyler^{a,b,*}, Weijia Kuang^b

^a Department of Astronomy, University of Maryland, College Park, United States

^b Planetary Geodynamics Laboratory, NASA Goddard Space Flight Center, Code 698, Greenbelt, MD 20771, United States

ARTICLE INFO

Article history:

Received 13 February 2013

Received in revised form 9 October 2013

Accepted 11 March 2014

Available online 28 March 2014

Keywords:

Earth's core

Tidal dissipation

Geodynamo

Geophysical fluid dynamics

ABSTRACT

It has long been speculated that there is a stably stratified layer below the core-mantle boundary, and two recent studies have improved the constraints on the parameters describing this stratification. Here we consider the dynamical implications of this layer using a simplified model. We first show that the stratification in this surface layer has sensitive control over the rate at which tidal energy is transferred to the core. We then show that when the stratification parameters from the recent studies are used in this model, a resonant configuration arrives whereby tidal forces perform elevated rates of work in exciting core flow. Specifically, the internal wave speed derived from the two independent studies (150 and 155 m/s) are in remarkable agreement with the speed (152 m/s) required for excitation of the primary normal mode of oscillation as calculated from full solutions of the Laplace Tidal Equations applied to a reduced-gravity idealized model representing the stratified layer. In evaluating this agreement it is noteworthy that the idealized model assumed may be regarded as the most reduced representation of the stratified dynamics of the layer, in that there are no non-essential dynamical terms in the governing equations assumed. While it is certainly possible that a more realistic treatment may require additional dynamical terms or coupling, it is also clear that this reduced representation includes no freedom for coercing the correlation described. This suggests that one must accept either (1) that tidal forces resonantly excite core flow and this is predicted by a simple model or (2) that either the independent estimates or the dynamical model does not accurately portray the core surface layer and there has simply been an unlikely coincidence between three estimates of a stratification parameter which would otherwise have a broad plausible range.

© 2014 Elsevier B.V. All rights reserved.

1. Introduction

The region of the core-mantle boundary (CMB) is central in controlling the flux of energy and momentum into or out of the Earth's fluid core and has therefore been of great interest in a wide variety of geophysical studies. Various conjectures and observational inferences have been made regarding the structure of this region and in particular there has been debate over the mass density stratification of a thin layer near the top of the fluid core and the associated dynamical implications and constraints. It has been understood since long that this stratified layer will support internal waves, but the conditions for the resonant forcing of these waves by tidal forces has not been adequately addressed. The purpose of this paper is to provide these conditions using dynamically consistent solutions of the full Laplace Tidal Equations (LTE). A preli-

minary matter is to review proposed estimates or constraints describing the stratification parameters of this layer, as these parameters control the propagation speed (s) of the internal waves, and thereby the degree of resonance.

The stratified layer was initially proposed from geochemical experiments (Higgins and Kennedy, 1971) and consideration of the thermo-chemical evolution (Gubbins et al., 1982). While these and closely related later studies have been important in the postulation of the stratified layer, usefully constrained estimates of the stratification parameters were not obtained. The results can be collectively summarized as the expectation that the Brunt–Vaisala (buoyancy) frequency N is typically of the order of the rotation frequency (or less), and that the thickness h of the stratified layer is several 10's to 100's of kilometers. Within continuous-stratification models of the assumed dynamics, one might estimate the internal wave speed as $c \approx Nh$ (e.g. Braginsky, 1998), implying that c is several 10's m/s or less. Within a two-layer model under the limit where the lower layer is much larger than the upper layer (a so-called 1.5-layer model such as adopted in this study), $c = (g'h)^{1/2}$. This is the same expression as the shallow-water wave speed of a

* Corresponding author at: Planetary Geodynamics Laboratory, NASA Goddard Space Flight Center, Code 698, Greenbelt, MD 20771, United States. Tel.: +1 (301) 614 6472; fax: +1 (301) 614 65224.

E-mail address: robert.h.tyler@nasa.gov (R.H. Tyler).

thin, homogenous fluid, with the exception that the gravitational acceleration g has been replaced by the “reduced gravity” $g' = \frac{\Delta\rho}{\rho}g$, where $\Delta\rho/\rho$ is the fractional density difference between the two layers. Estimates of c using this approach, where possible, provide results roughly consistent with the above. A recent study (Gubbins and Davies, 2013) of a stratified layer maintained by barodiffusion of oxygen, sulfur and silicon provides an estimate for N reaching $N = 1.5 \times 10^{-3} \text{ s}^{-1}$ and $h = 100 \text{ km}$, from which $c \approx Nh = 150 \text{ m/s}$.

Further early attempts to describe the stratified layer came through studies of the geomagnetic secular variation and the convection required in driving the geodynamo. Inversion of observations of geomagnetic secular variation provides a description of flow at the top of the core from which constraints on the description of this stratified layer have been obtained (e.g. Whaler, 1980). Inferences drawn from this type of study are, however, highly contingent on the approximations and specific assumptions used in the core flow inversion, and on the limited geomagnetic data. Inferences have also been drawn through the operation of numerical dynamo simulations involving the stratified layer (Nakagawa, 2011; Stanley and Mohammadi, 2008). In such studies, the layer thickness and the density difference are arbitrary, and their dynamical consequences are clearly shown in the properties of the generated magnetic field at the CMB. But it is also understood that any inference of the realistic situation is indirect because the parameter domains in these numerical simulations are very limited and far away from that of the Earth's core. While these dynamo simulations provide qualitative information of the process of the geodynamo and perhaps its dependence on the stratified layer, they do not yet provide strong quantitative constraints describing the realistic properties of the layer.

Stratification parameters have been obtained more recently from analyses of seismic wave forms. Using the reduced-gravity approach together with the values described in (Lay and Young, 1990) of $\Delta\rho/\rho \sim 0.01$ and $h \sim 50 - 100 \text{ (km)}$, and assuming $g \approx 10.7 \text{ m/s}^2$ (Braginsky, 2000), produces $c \sim 73 - 103 \text{ (m/s)}$. A very recent study (Helffrich and Kaneshima, 2010) indicates the presence of a substantially thick stably stratified layer in the fluid core directly below the CMB. In supplementary online information provided with the cited study, the layer (h) was estimated to be 300 km thick and 7.5 parts per thousand less dense than the fluid below (i.e. $\Delta\rho/\rho \sim 0.0075$). These parameters produce $c = 155 \text{ m/s}$.

This tidal energy transfer rate will be greatly enhanced if internal waves in the stratified layer are resonantly excited by tidal forces. For this to occur, there must be a near match in both frequency and spatial pattern between at least one of the tidal forces and at least one of the stratified layer's natural modes of oscillation. While the tidal forces may be prescribed from astronomical parameters, the layer's natural modes depend on the stratification parameters. To discover if there is a match we may then, for each of the important tidal force constituents, take the spatial structure and frequency as prescribed and calculate the stratification parameters that would be needed to produce a resonant response to the tidal force. More specifically, the approach followed in this study is to treat the stratification parameter c as a free parameter, and through repeated solution we construct a description of the dependence of the tidal response on this parameter. This theoretical description of the stratification dependence of the transfer rate of tidal energy to the stratified core is the primary independent result of this study. Secondly, by comparing these results with the stratification estimates reviewed above, we draw inferences about the tidal state in the CMB layer. These second results obviously depend on the validity of the stratification-parameter estimates which show the range described above. We note that the two most recent estimates show a remarkably similar result for c obtained using quite different methods ($c = 155 \text{ m/s}$ (Helffrich and Kaneshima,

2010), and $c = 150 \text{ m/s}$ (Gubbins and Davies, 2013)). While we do not think this agreement provides confirmation of the parameter value, we shall take from this $c = 1.5 \times 10^2 \text{ m/s}$ as representing the best current estimate.

The outline of this paper is as follows: The following Section 2 is somewhat lengthy and primarily directed at providing the formulation and intuition behind the use of the 1.5-layer model. While this formulation is widely used in the dynamics of the stratified ocean and atmospheres, it is perhaps less well understood among the community investigating core flow. Those readers familiar with the class of “equivalent barotropic” models used to describe the dynamics of stratified fluids, might scan or skip this section. The section aims to describe the assumptions by which the Laplace Tidal Equations for an unstratified fluid (Hough, 1898) can be extended to the stratified case by simply changing the interpretation of some variables and parameters: For the 1.5-layer version chosen to model the dynamics within the stratified layer below the CMB, the shallow-water wave speed c is replaced by the reduced-gravity version (as described above in this section), the fluid momentum vector refers to only the flow in the thin upper layer, and the consequence of tangential flow convergence is to depress the lower interface of the layer (rather than lift the upper surface). The method for solving the LTE can be summarized here as a semi-analytical method that analytically decomposes the LTE into spherical-harmonic bases and performs a numerical inversion to obtain the associated coefficients. The results obtained using this model and method are described in Section 3. These theoretical results for the tidal solution are presented as a function of two unknown parameters. The imposition of potentially realistic parameters to select the appropriate solution scenario is performed in Section 4, and conclusions from this work are described in Section 5.

2. Model and method

The calculation of the required conditions for resonance is accessed through a mathematical model of the assumed dynamics in the surficial core. The *model* comprises these dynamical equations and assumptions. The *method* prescribes the strategy for obtaining solutions from the model. The equations assumed to govern the tidal dynamics within the thin layer are the Laplace Tidal Equations (LTE) including tidal forcing and dissipation terms. The LTE can be regarded as statements of conservation of momentum and mass appropriate for a thin layer. The name is of historical interest as these equations are not restricted to tidal applications. Indeed, the LTE are largely equivalent to the horizontal components of the linearized Navier–Stokes equations which show the inertial + rotational accelerations balanced by a pressure gradient, plus force and dissipation terms. What distinguishes the LTE from the linearized Navier–Stokes equations is the assumption that the pressure function involved can be described such that the vertical and horizontal components of the momentum equation are separable. This separability is required in Classical Tidal Theory (Lindzen and Chapman, 1969), and more generally forms the basis in geophysical fluid dynamics for separating external and internal modes. The separation constant between the LTE and the equation (s) describing the vertical structure are the wave speeds $c_{(i)}$ associated with the suite of modes indexed as (i) . (In the approach here there is only one mode (the first baroclinic mode) retained, and therefore the index (i) is discarded.) Because c shall be treated as a free parameter, the LTE solution set calculated from the plausible range of c then provides a complete set of tidal scenarios that is independent of the specific assumptions regarding the vertical structure. Indeed a variety of layer (as in the case used in this study) or continuous-stratification models may be applied for the

vertical structure of the CMB layer that produce similar values for the first baroclinic mode c . The LTE results depend only on c , and not on the model or observations used to produce c . Consideration of the vertical structure is only needed to infer the realistic c from observations or other descriptions of the stably stratified layer.

The equations solved are then those describing the horizontal (tangential) dependence of the linearized Navier–Stokes equations under “long-wave” or “thin-shell” assumptions, and with the vertical (radial) dependence parametrized through c . The layer is appropriately “thin” if the tangential length scales considered are much greater than the radial length scale, which can be taken to be the thickness of the layer (for barotropic modes) or the “equivalent depth,” “scale height,” or other application-dependent appropriate measure in the case of baroclinic modes. Because the terms “barotropic” and “baroclinic,” are persistently elected as jargon, let us provide here some separate clarification in the next paragraph, proceeding then with our discussion of the model in the paragraph following.

The terms “barotropic” and “baroclinic” are standard terms that have historical roots within the literature of geophysical and astrophysical fluid dynamics. They originally referred to the alignment (*trope*) or misalignment (*cline*) of constant density and pressure surfaces. The reference to modes associated with each may be seen as a recognition of mathematical separability within idealized governing equations in which a stratified fluid has one barotropic mode as well as a potentially infinite suite of baroclinic modes describing the propagation of internal waves within the fluid. The barotropic or “external” wave is perhaps the more intuitive of the two and ocean swell or tides are a familiar example. The reader may have seen examples of a clear container containing two immiscible fluids (i.e. there are only two fluid densities involved). Such a fluid supports only one baroclinic mode, and such containers are sometimes built to demonstrate this internal wave active at the interface between the two fluids. If the upper surface is not constrained by the container, the fluid supports also a barotropic mode and therefore simultaneously supports two types of waves. It is often the case that the density difference between the two fluids is much smaller than the density difference between either and the atmosphere (another fluid which may be ignored so long as its density is indeed much smaller). As a result, the internal wave is seen to propagate relatively slowly and, as in the discussion below, one may restore some intuition by referring to this as a “reduced gravity” or “equivalent barotropic” mode when the adjustment to the governing equations can be made simply by replacing the usual gravity constant with one weighted by the fractional density difference between the fluids. When the fluid has more layers or is regarded as continuously stratified, there can be more than one baroclinic mode, but it is often the case that only the lowest modes need be considered. It is generally the case that the baroclinic modes of a fluid propagate more slowly than the barotropic mode. A few extensions to this discussion of the two wave varieties existing in the clear container may be helpful in following the arguments presented below:

First, one may have the baroclinic mode even if there is no free surface but rather a rigid lid. If this is not immediately clear, consider the following thought experiment. If the container is initially at rest, the interface between the fluids is presumably a horizontal (geopotential) surface. If one then tilts the container, it is not to be expected that the interface remains as it was but rather that after some transient adjustment a new equilibrium is reached in which the interface is again aligned with a geopotential surface—independent of the orientation of the container boundaries. If one rocks the container periodically, one may be able to establish through trial the frequency of the natural mode of oscillation of this baroclinic mode. Evidently, rocking at this frequency is more systematic at increasing the wave amplitude, while at other frequencies some

of the work performed may actually be working to decelerate the oscillation.

The effect we analyze in this paper is very closely related to determining the conditions for which there will be such a resonant match. In this case the forcing frequencies are set by the astronomical parameters, and the “container” dimensions and other constants are also set. Within the spherical geometry, one might loosely understand the condition for resonance as a situation where the wave speed is similar in amplitude (or an integer fraction) to the Earth’s equatorial rotation speed at the core such that the propagating phase of the responding medium matches that of the tidal forcing. The task is then to determine the range of stratification parameters (density difference and relative layer thicknesses) that allow for resonant forcing. Just as in the case of the simple container, the propagation speed of the internal wave depends on the stratification parameters. Very much unlike the case of a simple container, the propagation speed also depends on rotation, and the wave established—while still an oscillation—need not resemble the simple case. Indeed, it can be shown from scaling analyses of the governing equations that when considering the diurnal or semidiurnal tidal frequencies, the inertial and rotational terms have similar amplitude and therefore it is always the case that the Coriolis force is a significant restoring force in the oscillations allowed. The contrary case, however, is possible. Indeed, a special class of waves exist for which the Coriolis force is the dominant restoring force and gravity essentially acts only in the hydrostatic sense. In short, although the “container” and wave modes supported are more complex in the application we consider in this paper, the question we are addressing is fairly simple and extends directly from the simpler case just described. It should be fully expected that a stratified layer at the top of the core supports internal waves and that there are derivable natural modes that can be resonantly forced. What now requires support is the description of the model and method selected for this derivation.

As described at the opening of the last paragraph, the model implements the Laplace Tidal Equations (LTE) which apply only to an assumed thin layer. This is expected to be the case for the thin dynamically active region above or within the stratified region at the top of the fluid core. While the LTE were originally developed to describe tides in a thin ocean of uniform density, the LTE have long been extended to apply to a variety of applications in geophysical and astrophysical fluid dynamics including both barotropic and baroclinic dynamics. Here, the LTE are adapted to the so-called “1.5-layer model.” In the 1.5-layer assumption, a thin, stably stratified surface layer is replaced with a thin light layer overlying an asymptotically thick denser layer. This crudely simple model has been used to study thin stratified layers in a wide range of applications ranging from the ocean’s mixed surface layer (LeBlond and Mysak, 1978; Pedlosky, 1979; Nof, 1981; Tyler and Käse, 2001) to a thin stratified surface layer in the atmosphere of Jupiter (Dowling and Ingersoll, 1989; Ingersoll et al., 2004). The primary advantage of the model is that only the longest wavelength internal waves are resolved and the Laplace Tidal Equations retain a simple form identical to that in an unstratified fluid. However, an important parameter in the equations, the shallow-water wave speed $c = (gh)^{1/2}$ describing the speed of propagation of free oscillations, is replaced by a form c_b that is dependent on the assumed stratification (the subscript “ b ” shall be from here on retained to emphasize this distinction). The 1.5-layer model can be regarded as the model within the class of “equivalent barotropic” models where this dependency of c_b on stratification is maximally simple: While the shallow-water wave speed for a thin unstratified fluid is given by $c = (gh)^{1/2}$, where g is the gravitational acceleration and h is the thickness of the layer, the corresponding c_b in the 1.5-layer model is simply $c_b = (g'h_1)^{1/2}$, with the only difference that g has been replaced by the “reduced gravity” $g' = \frac{\Delta\rho}{\rho_2}g$

($\frac{\Delta\rho}{\rho_2}$ is the fractional density difference between the layers) and subscripts 1 and 2 have been used to distinguish parameters associated with the upper and lower layers, respectively. Because this model, while often used in geophysical fluid dynamics, has not been typically applied to core flow, in the next sub-section we provide a more in-depth review of this model and further discuss its applicability to the stratified layer considered.

The general approach in the *method* used here to solve the LTE was developed by Longuet-Higgins (1968) and the specific method is identical to that described in several formatively similar applications involving calculation of ocean tides on satellites in the outer solar system (Tyler, 2008, 2009, 2011). One should note that even though the same equations are solved in these different applications, the flow solutions obtained may be qualitatively quite different because of the different parameters involved (controlling the values of coefficients in the partial-differential equations). For the application in this study, the important features of this method are that it is semi-analytical (there are no free “tunable” parameters associated with the numerics other than the truncation degree of the spherical-harmonic expansion), and that it is computationally very quick and efficient (70,000 ocean tidal solutions are computed to complete the dense parameter-space diagrams presented below in Fig. 1). Because the equations solved are linear, the solutions are also unique. The distinction between *model* and *method* described at the start of this section is helpful in guiding the discussion: Because the method has been previously discussed and involves a generic semi-analytical inversion of the LTE, we do not expect further discussion on the method is needed here. The appropriateness of the model (i.e. the expected ability of the 1.5-layer model and LTE to capture the tidal dynamics of the thin stratified layer at the top of the core), however, shall be further described next.

2.1. Thin-shell fluid dynamics (one-layer formulation)

Before describing the more general model of a multi-layer stratified fluid, let us first review the statements of mass and momentum conservation appropriate for a single, thin layer of fluid of homogeneous density, and in the simplest case involving a solid lower boundary and a free upper surface. Approximations reduce the intrinsically three-dimensional flow problem to one involving only two-dimensional variables reflecting the integrals over the thin layer. In spherical coordinates, we refer to the thin layer as a “thin shell,” which can be compared to the term “thin sheet” used in Cartesian coordinates.

The thin-shell approximation is based on the assumption that the shell thickness is much smaller than the horizontal scales of flow variability. From the tangential (also called “horizontal”) flow velocity \mathbf{u} we define the depth integrated flow momentum in the shell of thickness h and constant water density ρ_o as

$$\mathbf{s} = \int_h \rho_o \mathbf{u} dr \quad (1)$$

where dr is the radial (vertical) increment. We also describe the dynamic (i.e. disequilibrium) displacement of the free upper surface η above the equilibrium height η_F as $\eta - \eta_F$. In the simplest case, η_F may represent a mere static position of rest of the fluid surface. But in the tidal application, η_F may vary in time and space to represent the changing gravitational potential due to tidal variations and therefore represents the primary forcing agent. More generally, η_F represents the shape that the upper surface of the fluid would adopt when fully adjusted to hydrostatic equilibrium (η_F can therefore equally represent centripetal accelerations associated with rotation, upper boundary conditions, and other effects).

Written in terms of these variables, the Laplace tidal equations

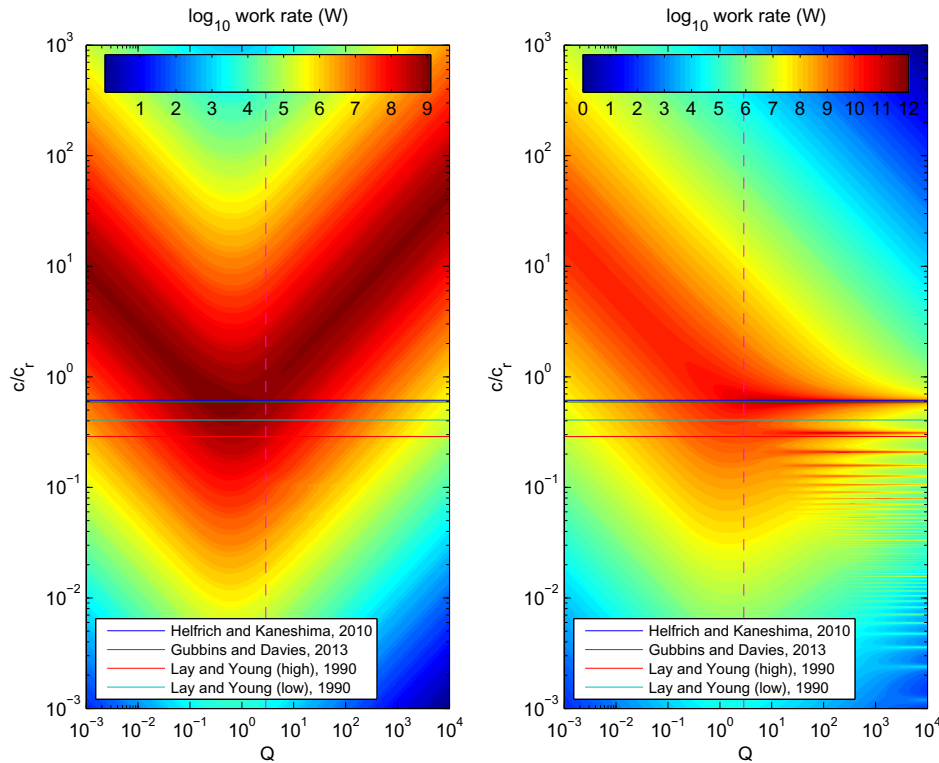


Fig. 1. Tidal rate of work (Log_{10} scale with a basis of 1 W) performed on the core fluid by the diurnal (left panel) and semidiurnal (right panel) tidal force constituents. Shown are in fact a space of solution scenarios as the rate of work depends on the imprecisely known dissipation Q and stratification c_b/c_r parameters. The horizontal lines show the value of $\frac{c_b}{c_r} = \frac{\rho_b}{\rho_r}$ assuming the “observed” stratification c_b derived from independent studies and in all cases indicate a semidiurnal tidal response in or near resonance; the two most recent estimates align very closely with the primary resonance peak (outside of the low- Q scenarios representing highly over-damped cases). The vertical dashed lines describe an estimate for the potentially realistic Q derived from the assumption of a Lorentz-force drag.

$$\partial_t(\rho_o \eta) + \nabla \cdot \mathbf{s} = 0 \quad (2)$$

$$(\partial_t + \alpha) \mathbf{s} - f \mathbf{s} \times \hat{\mathbf{r}} = -c^2 \nabla(\rho_o \eta - \rho_o \eta_F) \quad (3)$$

are statements of mass conservation (2) and momentum conservation (3) for a fluid in a thin shell. Above, $f = 2\Omega \cos(\theta)$ is the Coriolis parameter (with Ω the rotation rate and θ the colatitude), $\hat{\mathbf{r}}$ is the unit radial (vertical) vector, $c = (gh)^{1/2}$ is the shallow-water wave speed (g is the surface gravitational acceleration). The symbol α can be regarded as an operator describing the dissipation. In the simplest case, α is a constant (the operator is then just a multiplier) representing the Rayleigh friction coefficient. A subtle point is that solutions from these or similar equations can be used in a manner that does not require a belief that the dissipation process follow that of Rayleigh friction, or that is even similar. When, as in the approach in this study for example, the equations are solved repeatedly to fill in a solution space having as one of the free coordinates the parameter α (or a parameter dependent on this), then one may regard the Rayleigh term above as representing a generic so-far unspecified dissipation process. At the stage of examining the solution space, one may then impose the specification of a dissipation process by requiring that the allowed values of α carry a functional dependence on other parameters and perhaps even the solution variables. The selection of the dissipation process in this way selects a subset of the solution space as physically permitted. From an even more general viewpoint, one may regard the parameter α^{-1} as simply representing the time scale for removal of momentum from the system due to an unspecified process. Whatever the process (even if it is nonlinear), it surely has an associated time scale and one may use these simple linear equations to fill a large solution space spanning a range of all reasonable (and likely some unreasonable) values of α . The specification of the momentum-removal process then imposes a consistency constraint from which a subset of the solution space is permitted which may include solutions to linear or even non-linear dynamical process involving momentum transfer from the layer. At the stage of solution analyses in this study, we shall specify α to represent the effect of electromagnetic Lorentz forces whereby momentum is transferred from the active layer to surrounding conductive media through coupling by electric currents.

Note that the gradient term as well as the vector \mathbf{s} have only the two tangential components; the radial component of the momentum balance is assumed to be hydrostatically balanced and is implicitly included in this depth-integrated formulation. We also note that these equations as written are nonlinear because the pressure gradient term on the right hand side of (3) involves products of η and c^2 (c^2 is proportional to h which itself includes a contribution due to η). Other forms of these equations (e.g. involving depth averaged velocity instead of integrated momentum) may show the nonlinearity appearing in the mass conservation equation rather than the momentum equation, but the inherent nonlinearity is equivalent. The equations are immediately linearized by replacing the definition of the shallow water wave speed given above by $c \approx (gh_o)^{1/2}$, where h_o ignores the presumably small contribution of the surface displacement η to the total layer thickness.

Finally, we can rewrite (2) and (3) in a slightly different form that provides easier comparison in the later more general formulation involving the stratified fluid:

$$\partial_t(\rho_o h) + \nabla \cdot \mathbf{s} = 0 \quad (4)$$

$$(\partial_t + \alpha) \mathbf{s} - f \mathbf{s} \times \hat{\mathbf{r}} = -c^2 \nabla(\rho_o h - \rho_o H) \quad (5)$$

where H is the thickness of the fluid if it were in hydrostatic equilibrium. In the notation above, $H = h_o + \eta_F$.

2.2. Thin-shell fluid dynamics (multi-layer)

We shall now consider the general case of a stacked number of thin shells of fluid, while also removing some of the assumptions (e.g. free upper surface) made in the last section. We consider an arbitrary number K of shells labeled $k = 1 \dots K$, starting from the top shell of thickness h_1 and proceeding to the shell at the bottom of thickness h_K . The density ρ_k is assumed to be uniform within each layer. Any variations of ρ_k between layers must be monotonically increasing downward to maintain an assumed stable stratification.

Associated with each of these layers is also the equilibrium thicknesses $H_1 \dots H_K$ representing the thickness of each layer if the fluid were in hydrostatic equilibrium. Hence, away from solid lower or upper boundaries, H_k may represent the thickness between two geopotential surfaces and may be given a spatial/temporal dependence to reflect the tidal forces. Near a boundary, H_k may reflect the thickness between a geopotential surface and the location of the prescribed boundary. The hydrostatic pressure in each layer k is described as

$$P_k = P_{k-1} + g(\rho_k - \rho_{k-1}) \sum_{l=k}^K (h_l - H_l), \quad (6)$$

where the last term on the right-hand side of (6) describes the contribution due to the perturbed upper surface of the k th layer. The total hydrostatic pressure in layer k includes a contribution P_{k-1} describing the hydrostatic pressure exerted from the layers above. Physically, the pressure in layer k is due to the weight of all layers above, the only interesting part of which (P_k) is the contributions due to the dynamic displacements of the various layer interfaces. In other words, by “hydrostatic pressure” we are implicitly referring to only the dynamic component. For increased generality, let us also include a contribution p_k to describe a pressure contribution of unspecified non-hydrostatic origin. With these definitions, the equations for each layer k representing conservation of mass and momentum, respectively, are the following:

$$\partial_t(\rho_k h_k) + \nabla \cdot \mathbf{s}_k = 0 \quad (7)$$

$$(\partial_t + \alpha) \mathbf{s}_k - f \mathbf{s}_k \times \hat{\mathbf{r}} = -h_k \nabla(P_k + p_k). \quad (8)$$

This set of equations is inherently nonlinear because of the potential products of h_k and P_k (which is itself dependent on h_k through (6)). To linearize this set of equations, we may assume that the perturbations to the layer interfaces are small compared to the layer thickness such that the h_k appearing to the left of the gradient operator in (8) can be replaced by the time average of the prescribed equilibrium value, which we write as \bar{H}_k and which corresponds to the h_o used in the one-layer case. To explicitly distinguish the linearized form of the equations, as well as to provide notational convenience, let us define shallow-water wave speeds for each layer as $c_k = (g_k h_k)^{1/2}$, which involve the reduced gravity for each layer $g_k = \frac{(P_k - P_{k-1})}{\rho_k}$, and assume for the linearization that we have the valid approximation $c_k \approx (g_k \bar{H}_k)^{1/2}$. Combining these assumptions and using (6), the linearized governing equations are

$$\partial_t(\rho_k h_k) + \nabla \cdot \mathbf{s}_k = 0 \quad (9)$$

$$(\partial_t + \alpha) \mathbf{s}_k - f \mathbf{s}_k \times \hat{\mathbf{r}} = -c_k^2 \nabla(P_k + p_k)/g_k \quad (10)$$

$$P_k = P_{k-1} + g_k \rho_k \sum_{l=k}^K (h_l - H_l), \quad (11)$$

which form a closed set of linear equations, provided the dissipation α and non-hydrostatic pressure p_k terms are either ignored or commensurately prescribed.

2.2.1. The 1.5-layer model

The so-called 1.5-layer model is sometimes described as arriving from approximations appropriate for a two-layer fluid where the upper layer is thin and dynamically active, while the lower layer is very thick (infinitely thick) and quiescent. This description is, however, overly restrictive with regard to the layer thickness assumptions (as well as the number of assumed layers), and it is inadequate in describing what constitutes “dynamically active” because while flow speeds in the lower layer may be small, the integral momentum may be comparable to that in the upper layer. The approximation required for this model is nonetheless rather easy to describe:

A mathematical prescription for the 1.5-layer model can be obtained by assuming that the propagation speeds c_k for all layers $k > 1$ become infinite, while other terms in each of the k sets of momentum equations remain bounded. From this it is required that the pressure gradient on the right side of (10) in all layers $k > 1$ vanish. This can usually be combined with integral or boundary constraints to provide the statement which is the essential physical approximation assumed in this model: One assumes that whatever pressure $P_1 + p_1$ is created in the top layer h_1 is instantly compensated by the hydrostatic pressure associated with the displaced interface between h_1 and h_2 such that there is no net pressure on the layers below h_1 . One sees that the physical argument being made really has to do with adjustment time scales, or more specifically that the time scale for hydrostatic pressure adjustment in the lower layers is much faster than that in the thin top layer. Note that in the case of a solid upper boundary (a ceiling) on the fluid, there is no free upper surface on h_1 and one may indeed expect non-hydrostatic components p_1 to the pressure which may be communicated across the interface to lower layers. In any case, we need not specify the details of the pressure in h_1 for this model, only that it is compensated by the dynamic displacement of the lower interface of h_1 such that the pressure in h_2 vanishes (i.e. $P_2 + p_2 = 0$). Using this together with the assumption $p_2 = p_1$ (i.e. any non-hydrostatic pressure p_1 is communicated across the interface) in (11) provides

$$P_1 + p_1 = -g_2 \rho_2 (h_2 - H_2) \quad (12)$$

which states, as promised, that the pressure in layer 1 (left side) is compensated by the hydrostatic pressure associated with the interface displacement (right side) separating the layers h_1 and h_2 . Using this relationship in (9, 10) we obtain

$$\partial_t(\rho_1 h_1) + \nabla \cdot \mathbf{s}_1 = 0 \quad (13)$$

$$(\partial_t + \alpha) \mathbf{s}_1 - f \mathbf{s}_1 \times \hat{\mathbf{r}} = -c_b^2 \nabla (-\rho_1 \{h_1 - H_1\} + \rho_1 \{h - H\}), \quad (14)$$

where $c_b = \left(\left(\frac{\rho_2 - \rho_1}{\rho_2} \right) g h_1 \right)^{1/2}$ describes the speed of free propagation of the disturbed interface between h_1 and h_2 under the pressure-compensation assumptions.

The second term in curly brackets on the right side of (13) is exactly zero in the case of a solid upper boundary on the fluid because there is no free upper (or lower) surface; the total thickness h of the layer is then required to equal the total equilibrium thickness H describing the thickness between the upper and lower boundaries. Even in the case of a free upper surface of h_1 , this term may be omitted under the assumption that the dynamic displacement of the upper surface (equal to $h - H$) is small compared to the displacement of the lower surface. This assumption is a version of the so-called “rigid-lid” approximation. With this rigid-lid assumption and introducing the time-averaged equilibrium thickness \bar{H}_2 , let us define the variable $\eta_b = h_2 - \bar{H}_2$ to be the downward-positive dynamic displacement of the lower interface of layer 1 (the top layer), and similarly the equilibrium displacement $\eta_{bF} = H_2 - \bar{H}_2$. Substituting in (13, 14) we obtain

$$\partial_t(\rho_1 \eta_b) + \nabla \cdot \mathbf{s}_1 = 0 \quad (15)$$

$$(\partial_t + \alpha) \mathbf{s}_1 - f \mathbf{s}_1 \times \hat{\mathbf{r}} = -c_b^2 \nabla (\rho_1 \eta_b - \rho_1 \eta_{bF}), \quad (16)$$

which can be seen to be identical in form to the simplest equations (7, 8) governing a single layer. Aside from the subscripts indicating the variables are associated with layer 1, and the use of η_b to represent downward-positive displacements of the lower interface of the layer (rather than upward-positive displacements of the upper interface, as in η), the important difference is that the barotropic shallower-water wave speed c has been replaced by a baroclinic version c_b .

These 1.5-layer equations are in a family of so called “equivalent barotropic” equations because, while they patently describe baroclinic phenomena, they maintain a form equivalent to the barotropic equations described in (4, 5). Although the form of the equations is the same, the baroclinic wave speed c_b is typically much lower than the barotropic c in (4) leading to the characteristically slower speeds and time scales for baroclinic phenomena.

2.3. Application of the 1.5-layer model to the surficial core

We expect that the governing equations for the 1.5-layer model (13, 14) usefully describe the dynamics of a thin layer at the surface of the fluid core. More conservatively, we could claim that this formulation of the tidal dynamics of the CMB stratified layer is the useful form to start with because it is very likely the most reduced form possible with no expendable dynamical terms. This statement can be made rigorous through a scaling analysis of the various terms in the LTE assuming a diurnal time scale for the tidal forcing, and length scales comparable to an Earth radius. In this case, it is apparent that all terms (with the possible exception of the viscous/drag term involving the unknown parameter α) carry a comparable amplitude and therefore none can be discarded. One can, of course, argue that further terms are needed to capture other important dynamical effects. An obvious example would be a term representing electromagnetic Lorentz forces. While there is not a term explicitly representing this force, we consider its approximate representation through parametrization in the choice of α (or, alternatively, Q). In the latter case, an effective drag force is experienced in the active thin upper layer due to electromagnetic coupling with the lower layers. (We discuss this further below.)

As a simplification, we treat the CMB as rigid. In this case $h - H = 0$, h_1 varies only through displacements of the lower interface, and H_1 varies only with the tidal equilibrium height associated with this interface. The system of equations is then formatively identical to those solved in previous applications by one of the authors (Tyler, 2008, 2009, 2011).

The dominant tidal force for this application arises from the near 24-h rotation of the Earth with respect to either the Sun or Moon, or a “luni-solar” combination of the two having a nominal 24-h period. This near-diurnal period can appear as semidiurnal (≈ 12 -h) for tidal constituents having a spatial pattern with two peaks propagating along the same path. A generic description of these constituents is efficiently represented by the terms derived from an expansion of the time-varying gravitational potential using Associated Legendre Functions $P_n^s(\cos \theta)$ as a basis for the latitudinal dependence, which combine with an assumed sinusoidal basis for the longitudinal and temporal dependence to provide the spherical harmonic basis used in a wide variety of geophysical studies requiring representation of a variable over the surface of a sphere. Specifically, the gravitational potential is represented with a series of terms having the form $F_n^s P_n^s(\cos \theta) e^{-i(s\phi - \omega_F t)}$ where F_n^s describes a complex amplitude coefficient, θ is the colatitude, n is the degree, s is the order, ϕ is the longitude, ω_F is the frequency of the forcing constituent, and t is time. For the diurnal case

$n = 2$, $s = 1$, and $\omega_F = \Omega$ (where Ω is the rotation rate, as above). While for the semidiurnal case $n = 2$, $s = 2$, and $\omega_F = 2\Omega$. The amplitude F_n^s is also modulated by much lower frequency orbital variations and only representative constant values are used here as described below.

2.4. Post-processing solutions to obtain the total rate of work/dissipation

The solution of (13, 14) is obtained using the method described in detail in a previous publication (Tyler, 2011). As an element of the post-processing to obtain the work/dissipation rate associated with each solution, we make use of an energy equation. We derive this equation (defining $m = \rho_1 h_1$ and $m_F = \rho_1 H_1$ and otherwise dropping the layer subscript “1”) by taking the dot product of the flow velocity $\mathbf{u} = \mathbf{s}/(\rho h)$ with the momentum Eq. (14) which, with use of vector identities, can be written as

$$\partial_t \mathcal{E}_k + \nabla \cdot (\mathbf{F}_w) = \mathcal{W} - \mathcal{D}, \quad (17)$$

where $\mathcal{E}_k = \mathbf{s} \cdot \mathbf{s}/(2\rho h)$ is the kinetic energy density (energy per unit surface area on the globe), $\mathbf{F}_w = (m - m_F)g\rho^{-1}\mathbf{s} = (m - m_F)c^2\mathbf{u}$ is the flux of wave-field energy $(m - m_F)c^2$ due to advection by the flow, the rate of work done by tidal forces is $\mathcal{W} = -g\rho^{-1}(m - m_F)\partial_t m$, and the dissipation rate is $\mathcal{D} = -\alpha(\rho h)^{-1}\mathbf{s} \cdot \mathbf{s} = 2\alpha\mathcal{E}_k$. Other forms of this equation are possible because of the arbitrary reference level in defining potential energy density. A different form of the energy equation that can be derived by combining (17) with other relationships described above is

$$\partial_t (\mathcal{E}_k + \mathcal{E}_p) + \nabla \cdot (\mathbf{F}_w) = \mathcal{W} - \mathcal{D}, \quad (18)$$

where $\mathcal{E}_p = gm^2/(2\rho)$ and $\mathcal{W} = g\rho^{-1}m_F\partial_t m$ (other terms defined as above). Alternatively, we may take $\mathcal{E}_p = g(m - m_F)^2/(2\rho)$ and $\mathcal{W} = -g\rho^{-1}(m - m_F)\partial_t m_F$. As we see, the differences in these representations involve the reference level assumed in the definition of the potential energy \mathcal{E}_p . Note that while the definition of the work rate \mathcal{W} depends on the definition of potential energy, the global integral of \mathcal{W} averaged over a tidal cycle is equivalent in all forms and balances the integrated time-averaged \mathcal{D} .

3. Results

The tidal forces will generate a response in the thin layer below the CMB that may involve displacement of the lower interface (with associated potential energy) and/or fluid flow (with associated kinetic energy). The goal in showing solution results is to describe the conditions for which resonant forcing of the layer is achieved. There is no advance expectation for an equipartition of energy between these two forms, as may often be the case for waves generated in non-rotating fluids, and so an analysis in terms of just one of these solution quantities would be incomplete. The resonant response can, however, be reliably identified in the total rate of work done by the tidal forces on the fluid. This rate of work has units of power and describes the rate at which lunar/solar gravitational forces add energy to the core fluid.

In Fig. 1 we show results describing the rate of work performed by the primary diurnal and semidiurnal tidal-force constituents. This rate of work (integrated globally and averaged over a tidal cycle) appears as a function of two unknown parameters— Q (sometimes called the “quality factor”) and the ratio c_b/c_r . The Q factor is a dimensionless time scale describing the dissipation process and is defined as $Q = \omega_F \mathcal{E}_k / \mathcal{D}$, where \mathcal{E}_k and \mathcal{D} are respectively the globally-integrated time-averaged kinetic energy and dissipation rate of the system, and the forcing frequency ω_F is equal to the Earth’s rotation rate in the case of diurnal tidal forces, and twice this in the semidiurnal case (note $Q = \omega_F / (2\alpha)$). The ratio

c_b/c_r involves the stratification-dependent c_b (defined in Section 2 and equivalent to the reduced-gravity wave speed “ c ” described in the Introduction (Section 1) and the equatorial rotation speed (product of rotation rate and CMB radius) c_r . The ratio c_b/c_r may be regarded here as an axis describing the degree of stratification, with higher values of the ratio representing stronger stratification.

One may regard the solutions in Fig. 1 as a display of the full range of potential tidal scenarios. In fact, each plot is produced from over 70,000 separately calculated solutions, each assuming a unique pair $(Q, c_b/c_r)$. As we see, the rate of work done on the core fluid by tidal forces depends very strongly on the location of the configuration coordinates $(Q, c_b/c_r)$ relative to the various peaks in work rate seen. These maxima are of three primary types: The “picket fence” of narrow-band resonances in the lower right of the right panel in Fig. 1 describe resonantly excited waves in which the characteristic restoring force is gravity. These are sometimes referred to as “gravity waves” although this is inaccurate in that rotation (the Coriolis force) is just as important as a restoring force. In fact, rotation not only shifts the location of these resonance peaks but is responsible for the dispersion of energy over the many harmonic lines descending from the top-most primary peak. Without rotation there would be only one peak. The strength of these peaks increases with Q , while the bandwidth narrows and the resonance is more focused. The upper left of the right panel shows maxima associated with very viscous (creeping) flow. The solution in this region is analytically convergent with solutions that can be obtained easily from the governing equations in the simplified limit where inertial and Coriolis accelerations are ignored. A similar peak for low Q is seen in the diurnal case (left panel) but the region of high Q is quite different. The reason for this is well known. The resonance in this case describes excitation of long “planetary waves” rather than the “gravity” waves described above (Hough, 1898; Longuet-Higgins, 1968). These “gravity” and “planetary” waves are specifically the “Class I” and “Class II” oscillations appearing in more precise descriptions (Hough, 1898; Longuet-Higgins, 1968).

The work rate shown in Fig. 1 increases with the squared amplitude of the equilibrium height assumed for each tidal force component. At the Earth’s surface, the amplitudes for the primary lunar and solar equilibrium heights are roughly 0.24 m and 0.10 m, respectively, and one would find from simple downward continuation following an inverse-square dependence that the values at the CMB are roughly 0.07 m, and 0.03 m, respectively. Their combination to produce a luni-solar amplitude is not always given by the sum because their combination depends on the lunar and annual orbital phases, but to provide referential estimates for the dimensionalized amplitudes in Fig. 1, we assume these simply estimated values. A more accurate estimate for these tidal force amplitudes at the CMB would also require consideration and assumptions regarding the Earth’s tidal response. It is expected that the increased accuracy would affect only the scaled amplitudes of the results in Fig. 1 and not the positions of the resonances which are the primary result discussed here.

A simplification we have used which does shift the location of the resonance peaks is the assumption that the lunar and solar tidal forcing have the same base period of 24 h, when in fact the period associated with the lunar component is about four percent larger. Repeating the calculations with the lunar period provides very similar results that are largely indistinguishable from that in Fig. 1.

The solutions for the tidal response have so far only been discussed in terms of the rate of work performed. While this provides a description of the level of excitation in the stratified layer, it does not provide a kinematic description of the tidal flow response. This description of the flow vectors is not required in addressing the main points but we provide in the Appendix an example scenario

which shows that the flow is equatorially intensified with amplitudes of order 0.1 mm/s.

4. Comparison with observations

The horizontal lines in Fig. 1 describes the stratification of the surficial core according to the independent estimates for c reviewed in Section 1. (As described in Section 2.1, we refer to this parameter now as c_b to indicate that we have restricted interest to the wave speed of the first baroclinic mode. The solutions in Fig. 1 use the coordinate c/c_r in which c is generic and does not require this assumption.) The lines describes the value $c/c_r = c_b/c_r$ calculated using c_b from the independent studies.

One notices that the two most recent estimates (Helffrich and Kaneshima, 2010; Gubbins and Davies, 2013) are closely aligned with the primary resonance peak of the “picket fence” of peaks associated with rotational-gravity wave response. To produce $c_b = 155$ m/s from (Helffrich and Kaneshima, 2010), we use the definition $(c_b = (\frac{\Delta\rho}{\rho_2} gh_1)^{1/2})$ as discussed in Section 2) while assuming $\Delta\rho = 74\text{ kg/m}^3$, $\rho_2 = 9904\text{ kg/m}^3$ and $h_1 = 300$ km, which are the values described in the online Supplementary Information of the seismological study (Helffrich and Kaneshima, 2010). The value $\Delta\rho = 74\text{ kg/m}^2$ is described there as the “average density difference” at the bottom of page 12 and is the appropriate density difference to use in the depth averaged layer model here. The value for $c_b = 150$ m/s from (Gubbins and Davies, 2013) is obtained as $c_b = Nh$ (see Section 1) using the values for the buoyancy frequency N and layer depth h from that study. While we do not expect that the close match between the independent c_b estimates holds beyond the second significant decimal place, it does seem reasonable to assume that $c_b = 1.5 \times 10^2$ m/s is a most plausible estimate that aligns with the primary resonance peak. It would then follow that the surficial core is, to within the resolution that can be discussed, rather precisely in a state of resonant excitation by the semi-diurnal tidal forces. But the precision in this match should be further studied as it very likely exceeds the precision of the invested parts.

A potentially more robust conclusion is that for an assumption $c_b \leq 150$ m/s, one must contend with the possibility that the surficial core is in a resonantly excited state. Whereas for c_b appreciably greater than 155 m/s (and excluding the extremely over-damped low- Q scenarios), the tidal solution falls within the upper right of Fig. 1 (right panel) and one may assume that the semi-diurnal tides do not resonantly excite the layer. In the latter case there is still the potential for falling within the resonance peak associated with the diurnal tidal forcing (upper right of Fig. 1 (left panel)) but notice that the amplitudes of the work rate are much smaller than in the semi-diurnal case. In summary, the concern for resonantly excited states most applies for $c_b \leq 150$ m/s. This is relevant because the earlier estimates for c_b are lower than the recent values and so even if these lower values are preferred as more realistic, the conclusion in this paragraph that the CMB layer is in or near resonance still holds. The range $c_b = 73\text{--}103$ m/s inferred from (Lay and Young, 1990), for example, are at or near resonance with the primary and second harmonic peaks. Even between the peaks the response amplitude is elevated due to these resonances and so resonance is part of the response.

The model used in producing the resonance structure in Fig. 1 has idealizing assumptions. The most important is that it is assumed that the layer depth h is uniform and global. This is probably a reasonable assumption unless h is allowed to become as small as the expected departures of geopotential surfaces near the CMB from spherical surfaces. The conclusion regarding a resonant match is less sensitive to assumptions regarding the dissipation parameter Q as it can be seen that the relevant peak is

primarily horizontal in the diagram of Fig. 1 and therefore the rate of work is much less sensitive to Q assumptions. We can, however, provide an estimate of Q as follows:

The vertical dashed lines in Fig. 1 describe estimates for a potentially realistic Q which we derive from the approximate layer-integrated Lorentz force $-\frac{\sigma}{\rho} B_r^2 \mathbf{s}$ (where $\sigma = 10^6$ S/m, $\rho = \rho_1$, \mathbf{s} is the momentum integrated over depth h_1) assuming root-mean square radial magnetic field strength B_r at the CMB to be 5×10^{-4} T. In this case we assume the Lorentz force is the primary drag force in the dynamic layer h_1 . This approximation is given by the asymptotic limit of an infinitely thin layer under a perfect insulator and above a perfect conductor. In this case the Lorentz force $\mathbf{J} \times \mathbf{B} \approx (\sigma \rho^{-1} \mathbf{s}) \times (B_r \mathbf{r}) = -\frac{\sigma}{\rho} B_r^2 \mathbf{s}$ and one can see that this has the same form as the drag term in (14) provided the drag/attenuation coefficient is taken to be $\alpha = \frac{\sigma}{\rho} B_r^2$. By definition, Q is related to the attenuation as $Q = \omega_F / (2\alpha)$. Substituting the calculated α provides the vertical dashed lines in Fig. 1 at the location of $Q = 1.4$ (left panel) and $Q = 2.9$ (right panel). Note that because we are describing the behavior of the solution space using a full range of values for Q , it is not necessary to believe that Q arrives from a dissipation process similar to the one we have assumed for the calculations. Rather, the results are quite generic in that whatever dissipation process is active, the flow certainly has an associated Q because this simply is a non-dimensional time scale. A specified dissipation process prescribes the subset of this solution space that is allowed, and may be isolated by requiring that Q bear a relationship to other parameters or even the solution variables.

While these added assumptions regarding a choice of Q are not required in the main thesis of this paper, they motivate some interesting comments. Note that the fluid energy is directly converted to electric currents (magnetic energy), and the radial component of the magnetic field controls Q . This may suggest that the current configuration has stagnated at a position reflecting a balance where tidal energy is spent on potential energy (mixing to counter secular trends in stratification) and magnetic energy. While no direct method is apparent whereby this tidally generated magnetic energy will be organized into large-scale poloidal components, the resonant excitation mechanism should be more closely considered when looking for candidate energy sources affecting core processes. The dissipative heat would lead to rectified processes despite the periodic nature of the forcing and primary response elements. (There is also a rectification of the flow due to nonlinear action that may be expected. Estimates by extrapolation from the linear solutions obtained here indicate that this residual flow is, however, extremely weak).

Because the magnetic field holds, in this case, strong control over Q (increasing with the inverse square of the radial magnetic field strength), the transfer of tidal energy to a liquid core, as well as the evolution of its mass distribution (stratification), may depend sensitively on the strength of its magnetic field. Also, because the stratification is important in limiting convection, which in turn is important in controlling heat loss from the core, we see that these resonant processes may be important in both energy delivered and energy lost from the core.

5. Conclusions

There are both general and specific conclusions that can be drawn from these results. First, the diagrams in Fig. 1 are informative even if it were not known which ($Q, c/c_r$) coordinates correspond to the current or past situation for Earth. One can draw inferences from the paths describing an evolution through parameter coordinates and see where such paths must encounter resonance. If we assume that

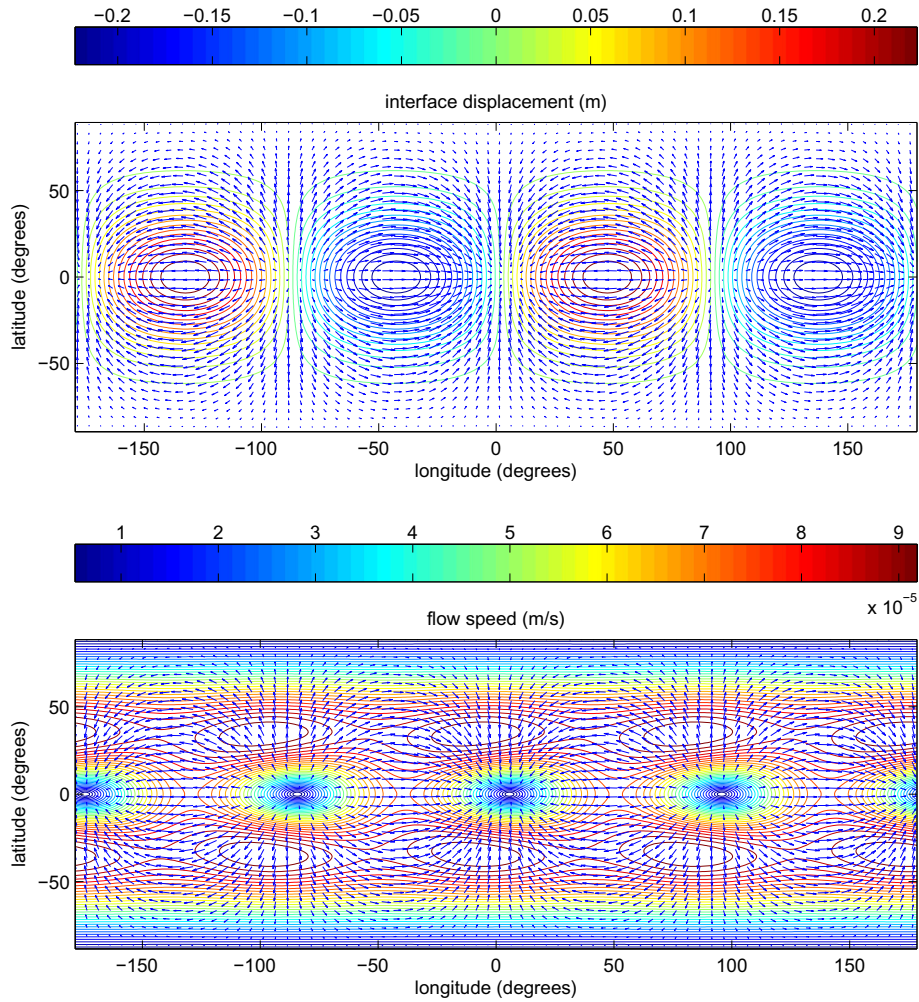


Fig. 2. Specific flow solution for the parameter coordinates described in text. Flow vectors appear above contours describing the interface displacement (top panel) and flow speed (bottom panel). Interface displacements are seen to be of amplitude 20 cm, while the flow speeds are 0.1 mm/s.

the surficial core was less stratified in the past (low c_b), for example, it has then moved upward in the diagram from a point below. The allowed path depends on the dissipation process assumed but it is important that there are significant resonance peaks spanning across the diagram that must be encountered for many or most paths involving vertical ascent to higher stratification. In such case, as the fluid attempts to stratify it is unavoidably pushed into a resonant state. The same type of encounter can be argued for paths of destratification or even horizontal paths of evolving Q . Most generally, we can argue that an evolving core requiring migration through points in these diagrams may typically encounter entry into resonance. If the entry into resonance slows or halts the migration, then a resonant configuration may be stable over long time periods. In this case, if the parameters ($Q, c/c_r$) are observed to be near a resonance peak this need not be accidental but may be a predictable result of negative feedback from the increased rate of work on the migration of the configuration through ($Q, c/c_r$) space.

Specific conclusions can be drawn using the independent constraints on the stratification parameter $c/c_r = c_b/c_r$. Immediately apparent through a wide range of Q is the close alignment of the “observed” (independently inferred) stratification parameters with those producing the primary resonance peak of the semidiurnal tide in the right panel of the diagram. This remarkably close alignment was discussed in the last section. (A broader alignment is also

observed for the diurnal tide in the left panel, but we shall focus from here on just the semidiurnal component.) This suggests that the CMB layer is currently in a resonantly excited tidal state.

A potentially more robust result that is independent of the other studies was also discussed in the last section: If the stratification parameters assumed are such that $c_b \lesssim 150$ m/s then one must consider the possibility of resonant forcing of the stratified layer by semi-diurnal tidal forces; if c_b is appreciably higher, one might justifiably ignore this possibility. Simple means for estimating c_b from other parameters are described in Sections 1 and 2.

The rate at which energy can be delivered to the core at or near these resonant configurations is seen to be significant. Near the primary resonance, the tidal work rate on the core is well above the levels associated with observed nutations (Buffett, 2010b,a) and can easily reach or even exceed the non-oceanic component of the total of tidal dissipation rate (Ray and Eanes, 2001) which is about 110 GW. Within the maximum of the resonance peak in Fig. 1 (right panel), the rate of energy transfer can exceed 0.1 TW and is therefore comparable to the work rate needed to sustain the geodynamo. Near the region where the dashed lines cross, the rate of work (and dissipation) is several tens of GW. Interestingly, this region also represents a special configuration close to critically damped ($Q = 1/2$), and there are related elements that have not been carefully considered here. One of the most widely known special features of the critically damped situation is that

the time for restoration to equilibrium is minimized (for this reason, such configurations are used in door stoppers and various circuitry where reduction of transients is desirable.) What may be of interest here, is that the critically-damped situation may behave as an attractor in configuration space and the present ($Q, c_b/c_r$) coordinates may be a derivable consequence of feedbacks. Such considerations are beyond the focus of this study.

The primary point in this paper is simply to show that independently derived estimates of stratification at the top of the core match theoretically derived requirements for the surficial core to become resonantly excited by tidal forces. As a direct consequence, the expected tidal energy input into the core is much greater than it would be otherwise. What becomes of this energy and its consequences on core dynamics requires further study. Further study of this potential process is relevant to both terrestrial and extraterrestrial dynamo processes.

Acknowledgements

The authors wish to thank Yves Rogister, Nick Schmerr, and two anonymous reviewers for their discussion and reviews of this manuscript.

For support, both authors thank the NASA Earth Surface and Interiors Program, and RT thanks the NASA Outer Planets Program.

Appendix A. A specific example of the flow field

The primary conclusions in this paper may not require precise knowledge about the realistic parameter c_b/c_r for the core, and knowledge of Q is even less required as the apparent proximity of the core's state with resonance conditions appears for all values of Q greater than the over-damped values. These primary conclusions are drawn from the behavior of the solution space as described by the time-averaged, globally-integrated work (or equivalently, dissipation) rate. One does, however, need the precise parameter coordinates in order to provide a description of the flow, or to describe the geographic distribution of the work or dissipation rates (though the integrals are equivalent, the distributions are not). Here it shall suffice to take these coordinates to be those described by the intersection in Fig. 1 of the vertical line (representing a realistic Q) and the horizontal line associated with the expected $c = c_b = 150$ m/s value. We shall restrict this description to the semidiurnal component.

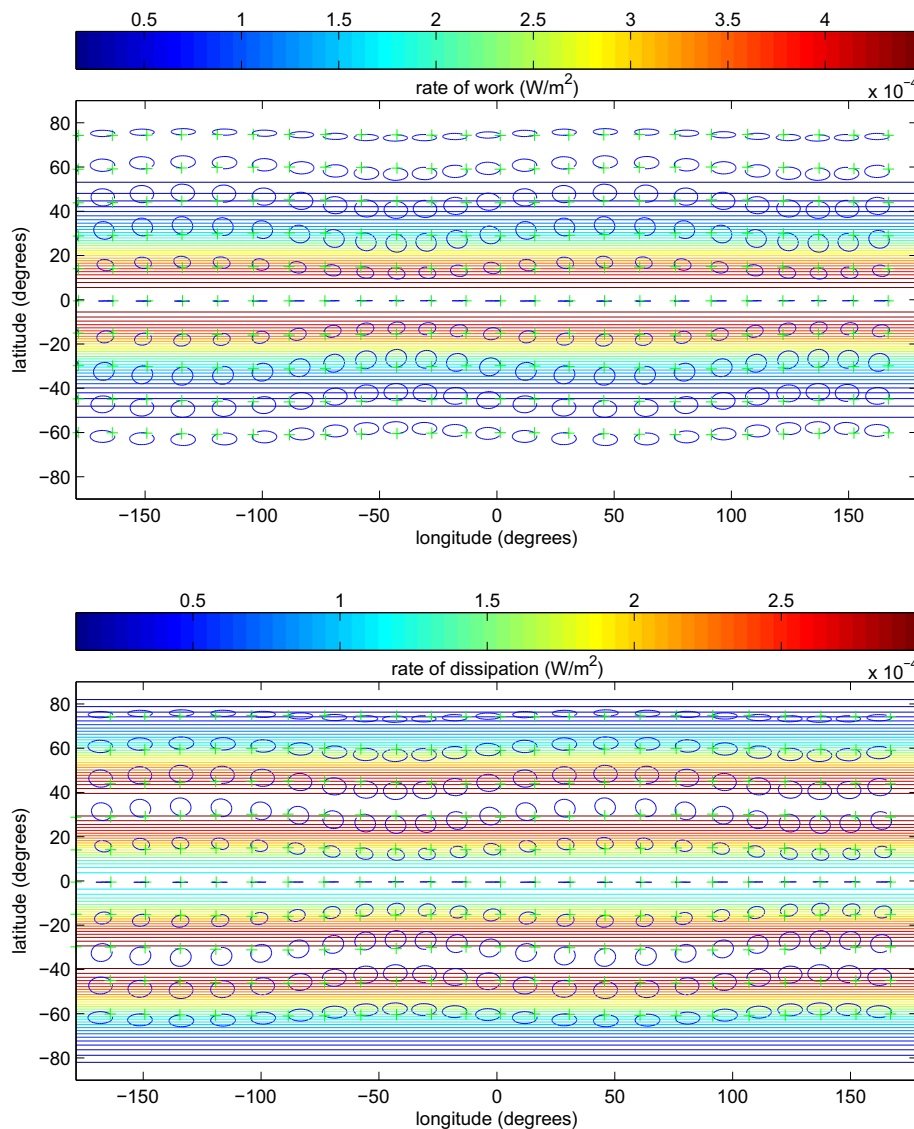


Fig. 3. Specific flow solution as in Fig. 2. Tidal ellipses (exaggerated flow trajectories, starting from green point) appear above the distributions of the rates of work (top panel) and dissipation (bottom panel).

In Fig. 2 we show the flow vectors and interface displacement. In Fig. 3 we show the tidal ellipses (the path of a fluid parcel over a tidal cycle) and the distribution of the rate of work and the rate of dissipation (W/m^2). All features propagate uniformly westward such that they travel around the core once per rotation period.

References

- Braginsky, S., 1998. Magnetic Rossby waves in the stratified ocean of the core, and topographic core-mantle coupling. *Earth Planets Space*.
- Braginsky, S., 2000. Effect of the stratified ocean of the core upon the Chandler wobble. *Phys. Earth Planet. Inter.* 118, 195–203.
- Buffett, B.A., 2010a. Tidal dissipation and the strength of the Earth's internal magnetic field. *Nature* 468, 952–954.
- Buffett, B.A., 2010b. Chemical stratification at the top of Earth's core: constraints from observations of nutations. *Earth Planet. Sci. Lett.* 296, 367–372.
- Dowling, T., Ingersoll, A.P., 1989. Jupiter's Great Red Spot as a shallow water system. *J. Atmos. Sci.* 46, 3256–3278.
- Gubbins, D., Davies, C.J., 2013. The stratified layer at the core-mantle boundary caused by barodiffusion of oxygen, sulphur and silicon. *Phys. Earth Planet. Inter.* 215, 21–28.
- Gubbins, D., Thomson, C.J., Whaler, K.A., 1982. Stable regions in the Earth's liquid core. *Geophys. J. Int.* 68, 241–251.
- Helffrich, G., Kaneshima, S., 2010. Outer-core compositional stratification from observed core wave speed profiles. *Nature* 468, 807–810.
- Higgins, G., Kennedy, G.C., 1971. The adiabatic gradient and the melting point gradient in the core of the Earth. *J. Geophys. Res.* 76, 1870.
- Hough, S., 1898. On the application of harmonic analyses to the dynamical theory of the tides. Part II: On the general integration of Laplace's dynamical equations. *Philos. Trans. R. Soc. London* 191, 139–185.
- Ingersoll, A.P. et al., 2004. Dynamics of Jupiter's atmosphere. In: *Jupiter: the Planet, Satellites and Magnetosphere*. Cambridge Planetary Science.
- Lay, T., Young, C.J., 1990. The stably-stratified outermost core revisited. *Geophys. Res. Lett.* 17, 2001–2004.
- LeBlond, P.H., Mysak, L.A., 1978. *Waves in the ocean*, Oceanography Series 20. Elsevier Scientific Publishing Company, Amsterdam, 602 pp.
- Lindzen, R., Chapman, S., 1969. Atmospheric tides. *Space Sci. Rev.* 10, 3–188.
- Longuet-Higgins, M., 1968. The eigenfunctions of Laplace's tidal equations over a sphere. *Philos. Trans. R. Soc. London* 262, 511–607.
- Nakagawa, T., 2011. Effect of a stably stratified layer near the outer boundary in numerical simulations of a magnetohydrodynamic dynamo in a rotating spherical shell and its implications for Earth's core. *Phys. Earth Planet. Inter.*, 1–11.
- Nof, D., 1981. On the β -induced movement of isolated baroclinic eddies. *J. Phys. Oceanogr.* 11, 1662–1672.
- Pedlosky, J., 1979. *Geophysical Fluid Dynamics*. Springer-Verlag, Berlin and New York, 710 pp.
- Ray, R., Eanes, R., 2001. Constraints on energy dissipation in the Earth's body tide from satellite tracking and altimetry. *Geophys. J.*
- Stanley, S., Mohammadi, A., 2008. Effects of an outer thin stably stratified layer on planetary dynamos. *Phys. Earth Planet. Inter.* 168, 179–190.
- Tyler, R., 2008. Strong ocean tidal flow and heating on moons of the outer planets. *Nature* 456, 770–772.
- Tyler, R., 2011. Tidal dynamical considerations constrain the state of an ocean on Enceladus. *Icarus* 211, 770–779.
- Tyler, R.H., 2009. Ocean tides heat Enceladus. *Geophys. Res. Lett.* 36, L15,205.
- Tyler, R.H., Käse, R., 2001. A 'string function' for describing the propagation of baroclinic energy anomalies such as eddies and rossby waves in the ocean. *J. Phys. Oceanogr.* 31, 765–776.
- Whaler, K.A., 1980. Does the whole of the Earth's core convect?.